Enhancement in free cooling potential through PCM based storage system integrated with direct evaporative cooling (DEC) unit

Panchabikesan, Karthik; Vincent, Antony Aroul Raj; Ding, Yulong; Ramalingam, Velraj

DOI:
10.1016/j.energy.2017.11.117

Document Version
Peer reviewed version

Citation for published version (Harvard):
Panchabikesan, K, Vincent, AAR, Ding, Y & Ramalingam, V 2018, 'Enhancement in free cooling potential through PCM based storage system integrated with direct evaporative cooling (DEC) unit', *Energy*, vol. 144, pp. 443-455. https://doi.org/10.1016/j.energy.2017.11.117

Accepted Manuscript

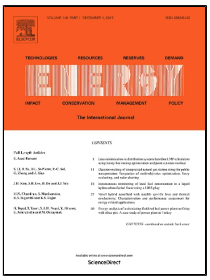

Enhancement in free cooling potential through PCM based storage system integrated with Direct Evaporative Cooling (DEC) unit

Karthik Panchabikesan, Antony Aroul Raj, Yulong Ding, Velraj Ramalingam

PII:	S0360-5442(17)31975-8
DOI:	10.1016/j.energy.2017.11.117
Reference:	EGY 11905
To appear in:	*Energy*
Received Date:	12 July 2017
Revised Date:	10 November 2017
Accepted Date:	20 November 2017

Please cite this article as: Karthik Panchabikesan, Antony Aroul Raj, Yulong Ding, Velraj Ramalingam, Enhancement in free cooling potential through PCM based storage system integrated with Direct Evaporative Cooling (DEC) unit, *Energy* (2017), doi: 10.1016/j.energy.2017.11.117

Highlights

- Proposed modified cooling system enhances the potential of PCM based free cooling.
- Freezing studies of an organic PCM is performed under real-time moderate climate.
- The proposed unit reduced the inlet HTF temperature by 2.35°C.
- 35% reduction in charging duration is achieved in modified cooling system.

Enhancement in free cooling potential through PCM based storage system integrated with Direct Evaporative Cooling (DEC) unit

Karthik Panchabikesan [a*], Antony Aroul Raj [b], Yulong Ding [c], Velraj Ramalingam [a]

[a] *Institute for Energy Studies, Anna University, Chennai, India 600025*
[b] *Department of Mechanical Engineering, Easwari Engineering College, Chennai, India 600089*
[c] *School of Chemical Engineering, University of Birmingham, Birmingham, United Kingdom B15 2TT*
[*] Corresponding Author: Karthik Panchabikesan (karthi0108@gmail.com)

Abstract

The present work reports the enhancement in free cooling potential using a modified cooling system compared to the conventional free cooling system. The proposed modified system is a novel pilot scale model packed with spherically encapsulated phase change material in the thermal energy storage tank along with water spray nozzles (direct evaporative cooling unit) at the inlet of the tank. The experiments were conducted in Bangalore, a city located in south India that possesses moderate/temperate climate throughout the year. Considering the local ambient conditions, an organic phase change material with the phase transition temperature range of 25.6 – 27.1 °C was used in the present study. Significant reduction in total charging duration and enhancement in heat transfer rate was achieved through the hybrid cooling system. The reduction in charging duration of 28.7 % and 34.8 % was observed for the proposed hybrid cooling system at heat transfer fluid (HTF) inlet velocities of 2 and 1.5 m/s respectively. It is observed from the results that in the experiments conducted with conventional free cooling system at 1m/s HTF velocity, the phase change material (PCM) placed in the last two rows of the storage tank did not reach its end freezing temperature even after 10 hours of experimentation due to the low heat transfer rate, whereas in the experiments conducted with the modified free cooling system, the storage tank is completely charged at all HTF velocities. It is construed from the results that the integration of evaporative cooling unit along with phase change material based free cooling system aids the chosen phase change material to completely solidify at a faster rate and augments the thermal performance of the storage unit. The proposed system can be operated as a single stand-alone cooling system to meet the cooling demand of the buildings or it can be integrated with the mechanically operated HVAC systems to achieve energy efficiency in the overall cooling system.

Keywords: Free cooling; Evaporative cooling; Thermal energy storage; Phase Change Material; Solidification behavior; Heat transfer rate;

1. Introduction

In India, 75% of the buildings that are anticipated by 2030 are still in the blue print stage and yet to be built [1]. This single data portrays the vital need for energy efficient buildings in the developing countries. Knowing the significant role of the building sector in managing a nation's energy demand, researchers around the world are working in every possible aspect to make a building energy efficient and eco-friendly. In recent years, use of PCM in buildings as a technology has transformed its application from research labs to commercial products. Depending on the

requirement of local climatic conditions, PCMs are either used for building cooling, heating, or both. Thermal comfort in a building using PCMs can be achieved by two methods, i) PCM integration in building envelopes/materials, and ii) PCM based free cooling. Both the methods depend on local climatic conditions and PCM phase change temperature range. The first method is a passive cooling method in which no additional storage place or mechanical equipment is required. In the second method, night time ambient air is circulated actively by using a fan/blower. The cold source freely available in HTF is used to charge the PCM and the stored energy in the PCM is retrieved during the daytime to reduce the temperature swing in the room. Since there is no energy spent to produce the cold source, this methodology is called as free cooling [2]. Both methodologies have its own advantages and disadvantages. The first method is a well matured and a commercialized technology. Whereas free cooling technology is not implemented widely compared to PCM integration in buildings.

The performance of PCM-based free cooling technology primarily depends on three parameters (a) local climatic condition, (b) PCM phase change temperature range and its thermophysical properties and (c) HTF inlet temperature/velocity and its thermophysical properties. The other parameters that influence the performance are encapsulation geometry/material, porosity/contact area between the PCM and HTF, fill volume, etc. Several review articles [3-9] were published in recent times that reported the influence of above said parameters on the thermal performance of the PCM-based free cooling system. The important inferences from the literature are i) places with minimum diurnal temperature variation of 15°C are highly suitable to implement the concept, ii) temperature driving potential of at least 3-4°C is required between PCM and HTF for efficient charging, discharging of energy, iii) PCM with appropriate phase change temperature in correspondence with local climatic conditions should be chosen and iv) if the temperature driving potential between the HTF and PCM is small, increasing the HTF velocity has only negligible impact on the charging process of PCM. Zalba et al. [10] analyzed the performance of the PCM-based free cooling system during both the charging and discharging process in a pilot scale model using the PCM with phase temperature range of 20 - 25°C. Their results showed that encapsulation thickness, HTF temperature/mass flow rate and the contact between PCM encapsulation/HTF significantly influences the performance of the system during both solidification and melting process.

Stritih and Butala [11] conducted a free cooling experiment using a pilot scale thermal energy storage (TES) system with 3.6 kg mass of PCM. The authors developed an equation for estimating the required solidification time with respect to HTF temperature/velocity and validated the equation with their experimental results. Antony and Velraj [12] investigated the charging process of RT 27 PCM for free cooling application in a heat exchanger based experimental setup. One of the major inferences from their study is the increase in tube side surface heat transfer coefficient in correspondence with the increase in HTF velocity. Arkar et al. [13] integrated the free cooling system into the ventilation system and analyzed the thermal response of a building using TRNSYS. The authors used spherically encapsulated RT 20 PCM for their analysis. They reported that for their case study, 6.4 kg of PCM/m^2 of floor area is optimum for the free cooling application. The

free cooling system resulted in energy savings through reducing the air flow rates during the night and it also reduced the noise associated problems [14]. The performance of free cooling system should be improved during the charging process in order to make the system competitive in terms of its operating cost as higher mass flow rate of air is required during the charging process [15]. Medved and Arkar [16] developed a correlation to estimate the free cooling potential based on the local climate. The authors reported that free cooling potential of a given location is proportional to the diurnal temperature range. Vidrih et al. [17] developed a generalized model based predictive weather control (G-MPWC) algorithm to predict the operational feasibility and efficiency of free cooling system for the next day. The G-MPWC was presented in the form of control matrixes based on the chosen building thermal response, free cooling system parameters and local weather data.

Mosaffa et al. [18] investigated the effect of HTF temperature and velocity on the charging process of multiple PCM based free cooling system. The major inference from their results is that, reducing the inlet HTF temperature than increasing the HTF flow rate during the charging process had a significant impact in increasing the exergy efficiency. Solomon et al. [19] analyzed the effect of sub-cooling during the charging of RT 21 PCM at different HTF temperature and velocities. It is reported that duration of sub-cooling is proportional to the heat flux. Lower the heat flux, lower the duration of the sub-cooling. Thambidurai et al. [20] experimentally analyzed the potential of free cooling application in reducing the room temperature during day hours. The experiments were conducted for the climatic condition of Pune city, India. Their results revealed that by extracting the useful stored energy in the PCM actively, 2.5°C drop in the designated room temperature was observed during the day time. Karthik et al. [8] estimated the annual cooling potential of the PCM-based free cooling system for five different cities of India. Their results indicated that city with moderate climate possessed higher cooling potential compared to other climatic zones. Considering the energy efficiency and potential of free cooling system in maintaining the room temperature, several recent research works have focused on improving the thermal performance of the TES system by introducing fin configurations, metal matrix and Lessing rings [21-27], dispersion of high conducting nanomaterials [28-30], increasing the PCM fill volume ratio [31] and by adopting high conductive encapsulation materials. Few works also have been carried out by the researchers by combining equivalent passive cooling concept such as evaporative cooling, nocturnal radiative cooling concept with the TES system and thereby increase the thermal performance of the whole system [32, 33] .

It is inferred from the literature that implementation of the PCM-based free cooling concept is recommended in the climatic zones that possess a high diurnal temperature and temperature driving potential. HTF Velocity/Temperature, PCM phase transition temperature range, and encapsulation geometry/material are the other parameters that influence the thermal performance of the free cooling system. Most of the studies found in the literature were performed under controlled conditions by simulating the ambient conditions. The data available on addressing the performance of the free cooling system under real time ambient conditions are scarcely found. It is also observed that all the studies reported in the literature were aimed at improving the thermal

performance of the thermal storage system by adopting the heat transfer enhancement techniques such as adding fin configurations, nanomaterials in the PCM, etc. As per the author's best knowledge, no research work has been reported in the literature to enhance the potential of free cooling by increasing the temperature driving potential between the PCM and HTF.

In the present work, the major novelty is the integration of PCM based storage system with the direct evaporative cooling (DEC) unit. An attempt is made to study the charging behavior of PCM-based free cooling system with and without the operation of water spray nozzles under real time moderate climate ambient conditions. The main aim is to report the enhancement achieved in the thermal performance of the PCM-based free cooling system when operated in conjunction with DEC unit. The experiments were conducted during the months of May-June in the Bangalore city, India and the results obtained are reported in the present paper.

2. Experimentation

2.1. Experimental setup

An experimental setup is constructed in a pilot scale that consists of a cylindrical tank, organic PCM encapsulated in high-density polyethylene (HDPE) spherical balls, an axial fan, water spray nozzles, centrifugal pump, water tank and resistance temperature detectors (RTD) sensors. The schematic diagram of the PCM based free cooling experimental setup with water spray nozzles is shown in Fig. 1 and the photographic representation of the fabricated setup is shown in Fig. 2. The TES tank is made up of two acrylic cylinders with outer diameter (OD) 245 mm, 5 mm thickness, and 600 mm height, which on assembling together forms a single vertical cylindrical tank of height 1200 mm in which height of the PCM test section is 450 mm. The PCM used in the present study is commercially available RT28 PCM (paraffin wax) with a high concentration of n-Docosane (C_{22} H_{46}). The differential scanning calorimetry (DSC) analysis of the chosen PCM was performed using Mettler Toledo - MT DSC2 instrument at a scanning rate of 0.5°C/min. The thermophysical properties of the PCM obtained from the manufacturer and the DSC analysis are given in Table 1 and Fig. 3. It is seen from Fig. 3 that the phase change occurs in the temperature range of 25.6 – 27.1°C and the peak transition phase change temperature of the PCM is observed at 27°C. In the TES tank, totally 49 HDPE spherical balls of OD 75 mm, 2mm thickness were arranged in 7 rows with 7 balls in each row. The PCM in liquid state was filled inside the HDPE balls with a fill volume ratio of 85%.

A perforated circular stainless-steel mesh positioned at a distance of 800 mm from the top of the tank is used to hold the PCM balls. The porosity of the TES tank after packing the spherically encapsulated PCM balls was found to be 39 %. The TES tank was insulated with 9 mm polyurethane foam sheets ($k = 0.03$ $W.m^{-1}.K^{-1}$) to minimize heat exchange between the storage tank and the ambient. An axial fan (9-inch diameter) with a capacity of 300 CFM driven by 60 W motor was placed over the top of TES tank to circulate the night time ambient air into the TES tank. The HTF velocity/mass flow rate is controlled by using a voltage regulator. The nozzles spray the water as a fine mist to completely saturate the air with respect to the local relative humidity (RH). For the given air flow rates, it is estimated that water flow rate of ~ 0.25 Gallons

per hour (GPH) is required to saturate the air to ~80% RH. A centrifugal pump with the pressure regulator was used to pump water from the water tank. In order to produce fine mists, water is pressurized up to 6 bar (cut-off pressure) and discharged through the spray nozzles. When the water pressure reaches 6 bar, pump operation shuts off and starts again once the pressure reaches 1.2 bar (cut in pressure). The pump was 'ON' only for 8 seconds in the 86 seconds ON - OFF cycle duration thereby avoiding the continuous operation and the consequent increase in water temperature.

The PCM temperature at each row, HTF inlet/outlet temperature, water and ambient air temperature were measured using 11 PT 100 RTDs (3 wire, accuracy ±0.1°C) and the locations of RTDs are shown in Fig. 1. The HP-Agilent 34970A, Data Acquisition System (DAS) was used to record the temperatures, at a scanning rate of 1 minute throughout the experiment. The RTD transducer temperature conversion accuracy of the data logger is ±0.02°C. Digital vane anemometer (Work Zone, AVM-03 model) with ± 3.0% accuracy and 0.1 m. s^{-1} resolution was used to measure the HTF velocities. At the beginning of each experiment, required flow rate of the HTF was attained by adjusting the fan regulator. The relative humidity of the HTF (both ambient and inside the TES) was measured using the digital hygro-thermometer with an accuracy of ± 3%.

"Fig. 1. Schematic diagram of modified free cooling system integrated with DEC unit"

"Fig. 2. Photographic views of **(a)** modified free cooling system without insulation, **(b)** water spray nozzle, **(c)** axial fan placed at the top of the TES tank, **(d)** Data acquisition system"

"Fig. 3. DSC Analysis of paraffin (RT 28 HC)"

"Table 1 Thermophysical properties of RT 28HC PCM [34]"

2.2. Experimental procedure

The charging experiments were conducted under two experimental configurations; with and without the operation of water spray nozzles at three different HTF velocities or mass flow rates (2m/s or 0.11 kg/s, 1.5 m/s or 0.08 kg/s and 1 m/s or 0.05 kg/s) respectively. In the first case, pump was kept OFF and the ambient air was circulated inside the TES tank as the HTF. In the second case, the pump was turned ON and OFF in a chosen intermittent frequency to cause the required water spray inside the TES tank wherein the evaporatively cooled moist and saturated air is the HTF. It is ensured that the phase change material in storage tank remained in liquid state within the temperature range of ~ 30.5°C – 32.0°C before the start of each experiment. The experiments were conducted during the night time from ~10.00 p.m. until the PCM gets completely charged or until once there was a noticeable rise in the ambient temperature after the sun rise. The TES tank is considered to be completely charged once the PCM in all rows reached 25.6°C (the end solidification temperature obtained from DSC analysis). All the experiments were repeated twice and the difference between the recorded data observed was to be negligible. Since the experiments were conducted under real time ambient conditions there was no control over the HTF temperature

and relative humidity. However, it is ensured that all the experiments were performed almost under similar ambient conditions with minimum deviations. The free cooling experiments conducted without and with the operation of DEC unit are hereafter referred as 'case I' and 'case II' respectively in this article.

3. Data reduction and Uncertainty analysis

The heat transfer coefficient *'h'* between the PCM balls and HTF in the storage tank was calculated using the Nusselt number correlation proposed by Felix et al. [35] and the same is presented in equation 1. The 'h' for the experiments performed under 'case I' was calculated by considering the properties of inlet HTF temperature at every time step, whereas for 'case II' experiments, 'h' was calculated by considering the HTF properties in correspondence to inlet temperature and relative humidity at every time step.

$$Nu = \frac{h * D_p}{k_{HTF}} = 2.0 + 1.1[6(1-\varepsilon)]^{0.6} * Re^{0.6} * Pr^{0.33} \quad (1)$$

Where,

$$D_p = {}^{6}\!/_{S_v}$$

$$S_v = \frac{Area\ of\ spherical\ ball}{Volume\ of\ spherical\ ball}$$

$$Re = \frac{D_p * v_s * \rho}{\mu}$$

$$Pr = \frac{c_{p,HTF} * \mu}{k_{HTF}}$$

The instantaneous heat transfer '$\dot{Q}_{ins}$' for the free cooling experiments conducted without and with DEC unit at every *'i^{th}'* time step was evaluated using equation 2 and 3 respectively.

$$\dot{Q}_{ins} = [\dot{m}_f \times c_{p,HTF} \times (T^{\,i}_{HTF,out} - T^{\,i}_{HTF,in}) - Q^{\,i}_{loss}] \quad (2)$$

$$\dot{Q}_{ins} = [\dot{m}_f \times (H^i_2 - H^i_1)] - Q^{\,i}_{loss} \quad (3)$$

The heat loss '$Q^{\,i}_{loss}$' between the air in the TES tank and ambient is evaluated using the equation 4.

$$Q^{\,i}_{loss} = \frac{k_{insulation} \times A_{TES\ section} \times \left(T^{\,i}_{ambient} - \left(\frac{T^{\,i}_{HTF,in} + T^{\,i}_{HTF,out}}{2} \right) \right)}{x} \quad (4)$$

The cumulative energy stored 'Q_c^i' during the experiments is calculated using the equation 5.

$$Q_c^i = \sum_{i=0}^{n} \dot{Q_{ins}} \times dt \quad (5)$$

During the experimentation, only the inlet and outlet temperature of the HTF were measured. In order to find the HTF temperature after each row of the TES tank, equation 6 is formulated.

$$T_{j+1,\ HTF}^{\ i} = \left\{ \frac{{}^{h}/_{1000} * A_{pcm} * n * \left(T_{pcm}^{\ i} - T_{j,\ HTF}^{\ i}\right)}{\dot{m}_f * c_{p,HTF}} \right\} + T_{j,\ HTF}^{\ i} \quad (6)$$

This temperature was used to calculate the percentage of total heat transfer rate at every row of the TES tank.

3.1. Uncertainty analysis

The error propagation method proposed by Strupstad [36] was used to estimate the uncertainty and the same are presented in Table 2. The errors involved in the measured and derived parameters were calculated based on the sensitivity/accuracy of the measuring instruments used in the present study and the minimum value of the measured parameters.

"Table 2 Uncertainty in measured and derived parameters"

4. Results and Discussion

In this section, results obtained from the charging experiments conducted with and without DEC unit under various HTF inlet air velocities are presented in terms of PCM solidification behavior, charging duration, instantaneous and cumulative heat transfer. Since inlet HTF temperature is one of the key factors influencing the charging process of PCM, its impact on the thermal performance of TES tank under different velocities is also discussed in detail. Among the various experimental trails, experiments conducted with 2 and 1.5 m/s HTF velocities under case II exhibited better thermal performance.

4.1. Variations in HTF inlet temperature

In the present study, charging experiments were carried out under the ambient conditions as shown in Table 3. The average ambient temperature and relative humidity recorded during the experimentation varied between 23.8°C – 24.7°C and 80.8% – 85.6% respectively. It is seen from Table 3 that the HTF temperature at the inlet of TES tank was 1.06°C, 1.29°C, 1.40°C higher than the ambient temperature for case I experiments whereas it was 2.25°C, 2.35°C, 1.36°C lesser than the ambient temperature in the case II experiments at the HTF velocities of 2, 1.5 and 1 m/s respectively. The increase in HTF temperature for the case I experiments is due to the heat generated by the continuous operation of the fan. Whereas in case II, spray of water particles into

the TES tank resulted in evaporative cooling and reduced the inlet HTF temperature up to its wet-bulb temperature depending on the local relative humidity. It is seen from Fig. 4 that during the experiments conducted as in the case I the HTF temperature at the inlet of TES tank varied from 27.6°C to 23.5°C in accordance with the ambient temperature. However, for the case II experiments, the HTF temperature at the inlet of TES tank remained in the near constant range of 23.7°C to 21.8°C for all the three HTF velocities irrespective of the ambient temperature. The reduction in HTF temperature for the case II experiments was due to the effect of evaporative cooling. The temperature difference between ambient and HTF critically influenced the charging process in terms of total charging duration and heat transfer rate between the two cases. In Fig.4, it is also to be noted that different trend in inlet HTF temperature is observed during the initial duration (50 – 100 min) of case II experiment conducted at 1 m/s HTF velocity. This is because, during the initial period of the case II experiment conducted at 1 m/s HTF velocity, inherent relative humidity of the ambient air increased from 80% to 87% compared to the other cases. Therefore, the potential for the temperature drop through evaporative cooling got reduced and this was reflected in the initial period of the experiment (50 -100 min) as the inlet HTF temperature rise.

"Table 3 Comparison of inlet HTF conditions for different experimental trials"

"Fig. 4. Variation in HTF inlet temperature at various HTF velocities"

4.2. PCM charging characteristics

The temperature history of the PCM along with the height of TES tank with respect to time during the charging experiments conducted in the case I and case II experimental configurations at various air velocities are shown in Fig. 5 and Fig. 6 respectively. The PCM located in the 1st row of TES tank is nearer to the entry of HTF and the 7th row PCM is farther from the entry of HTF. It is seen from Fig. 5 and Fig. 6 that PCM in all the rows of TES tank reached the solidification temperature (25.6°C obtained from DSC analysis) except in the case I experiment conducted at 1 m/s HTF velocity. This is because of the lower heat transfer rate at that particular experimental condition. In the case I experiments conducted at 1 m/s HTF velocity, after 612 minutes, the ambient temperature got increased as time progresses in the morning (after 06.15 a.m.). This increase in ambient temperature will be directly reflected in the inlet HTF temperature and subsequently the temperature of PCM in the TES tank will get increased. Hence continuing the experiment beyond 06.15 a.m. will lead to discharging of cool energy stored in the PCM. Therefore, the charging experiments were not extended further though the PCM placed in the 7th row of the TES tank was not completely charged. It is also observed that in case II experiments, the PCM reached its solidification temperature for all HTF velocities at a faster rate due to higher heat transfer rate compared to the case I experiments. Further, it is seen from figure 6 that in case II experiments conducted at 1.5 m/s HTF velocity, PCM placed in the initial six rows of TES tank reached its end freezing temperature at a faster rate compared to case II experiments conducted at

2 m/s HTF velocity. The possible reason for this could be the better air-water mixture ratio existed during the case II experiments at 2 m/s air velocity. It is construed from the results obtained that it is possible to achieve enhancement in PCM charging rate at a lower HTF velocities through the proposed hybrid system compared to the conventional free cooling system.

Few significant variations in the phase change temperature of chosen PCM were observed during the experimentation compared to the DSC results. It is observed from the DSC results that the major phase change of the PCM was between 27.1°C and 25.6°C, whereas during the experimentation, major phase change of the PCM occurred between the temperature range of ~ 29.5°C and ~ 28.1°C (solidification onset and end temperature) in case I and between the temperature range of ~ 29.3°C and ~ 27.8 °C in the case II as shown in Fig. 7. The possible reasons for this discrepancy between DSC and experimentation are; the start of freezing in the case of DSC analysis was much lower than the melting of the PCM as seen in Fig. 3. This is due to the absence of nucleating agents during the solidification process of DSC analysis. However, during the experimentations, surface roughness of the container itself acted as the nucleating agent and initiated the solidification of PCM. Thus, the freezing of the chosen PCM was initiated at near melting temperature of ~ 29 °C during the experimentation. Further, there is a noticeable shift in the start of solidification process between the case I and case II experiments and also in the PCM along the height of TES tank in both the cases. This is because the PCM located at the top of the TES tank was subjected to faster cooling rate and hence there is a marginal subcooling of PCM compared to the PCM located in the bottom of TES tank which is subjected to lower cooling rate. Also, a small difference in temperature observed at the start of phase change process between the case I and case II experiments were also due to the higher cooling rate in the case II experiments compared to the case I experiments.

"Fig. 5. Temperature-time history of PCM for the free cooling experiments conducted without the operation of DEC unit (a) 2 m/s velocity, (b) 1.5 m/s velocity, (c) 1 m/s velocity"

"Fig. 6. Temperature-time history of PCM for the free cooling experiments conducted with the operation of DEC unit (a) 2 m/s velocity, (b) 1.5 m/s velocity, (c) 1 m/s velocity"

"Fig. 7. Onset (T_l) and solidification (T_s) temperature of the chosen PCM obtained during the case I and II experimentations at 2, 1.5 and 1 m/s inlet HTF velocities"

4.3. Charging duration

The TES system is considered to be completely charged when all the encapsulated PCM placed in the last row of the storage tank reaches its end freezing temperature (25.6°C). Though the actual phase change of the chosen PCM initiated and completed much earlier during the experimentations compared to the DSC analysis, the end solidification temperature of the PCM obtained from DSC

results was considered in the present study. This consideration ensures the complete solidification of PCM and will be very useful to compare the performance of the case I and case II experiments. The charging duration of the PCM located at the last row of TES tank in both the cases is shown in Fig. 8. Since the PCM located at the 7th row of TES tank did not reach its end freezing temperature in the case I experiment at 1 m/s HTF velocity even after 10 hours of experimentation, its charging duration is not shown in Fig. 8. It is seen from the figure that charging duration in case II experiments was found to be 28.7% and 34.8% lower than the case I experiments at 2 and 1.5 m/s HTF velocities respectively. This is due to the appreciable drop in the inlet HTF temperature in the case II experiments as shown in Table 3. It is also observed from the table that enhancement in convective heat transfer coefficient after increasing the HTF velocity from 1.5 to 2 m/s was found to be in the range of 15% for both the cases. Though this enhancement in 'h' was similar in both the cases, increase in HTF velocity in the case II experiments showed only a marginal reduction of 5.5% in charging duration compared to the case I experiments wherein the reduction in charging duration of 13.3% was observed. This is because the increase in 'h' value as in the case II experiments have only minimal effect on the overall enhancement in the heat transfer rate. However, it is to be noted that whenever the surface convective resistance is dominant than the internal conductive resistance, increasing the HTF velocity has an appreciable effect for a longer duration during the initial period of charging. Thus, it is construed from the present results that reduction in the HTF temperature has a significant impact on the PCM solidification behavior than increasing the HTF velocity and convective heat transfer coefficient.

"Fig. 8. Charging duration of the PCM placed at the last row of TES tank"

4.4. Instantaneous heat transfer ($\dot{Q}_{ins}$)

The instantaneous heat transfer is an important parameter that directly depicts the thermal performance of the latent heat storage system with respect to thermophysical properties of the inlet HTF and PCM. Fig. 9 (a) and (b) show the variation in the instantaneous heat transfer rate evaluated using Eq. 2 and 3 for the case I and case II experiments respectively. In the case II experiments, inlet air becomes fully saturated and therefore its thermophysical properties varied compared to the ambient air. Hence Q_{ins} in case II experiments was calculated by considering the HTF inlet and outlet enthalpies at every ith time step. The average instantaneous heat transfer rate for the case I and case II experiments conducted at the HTF velocities of 2, 1.5, and 1 m/s were found to be 0.06 kW, 0.05 kW, 0.03 kW and 0.10 kW, 0.09 kW, 0.07 kW respectively. It is seen from Fig. 9 that there are continuous fluctuations in instantaneous heat transfer in the case II experiments. This is due to the fluctuations in the HTF temperature caused by the intermittent discharge of water particles from the spray nozzles. Though the air flow rate at the entry of TES tanks was maintained at a constant rate throughout the experiment, discharge of water as fine mists from the water spray nozzles kept varying based on the pump pressure. Initially, when the pump was operated at 6 bar pressure (cut in pressure) there was a complete discharge of water mists from the spray nozzles. Once the pump pressure tends to reach 1.2 bar (cut in pressure) the quantity of

water sprayed was minimal and hence the inlet HTF temperature kept varying marginally during each cycle of pump operation. This variation in HTF temperature was reflected in the instantaneous heat transfer in the case II experiments.

It is also seen from the figure that during the initial period of charging, instantaneous heat transfer decreased at a faster rate in both the experimental cases. This period denotes the sensible cooling process before the initiation of the charging of PCM. Once the latent cooling process was initiated, Q_{ins} remained in a near-constant range for a longer duration. In the case I experiments, only the increase in HTF velocity aided to improve the instantaneous heat transfer, whereas in case II experiments, the appreciable variation in thermophysical properties of air due to saturation that increased the temperature driving potential between PCM and HTF contributed predominantly in enhancing the instantaneous heat transfer along with the increase in HTF velocity.

"Fig. 9. Instantaneous heat transfer at various HTF velocities for (a) case I experiments (b) case II experiments"

4.5. Cumulative energy stored

Fig. 10 shows the cumulative thermal energy stored during the experiments conducted in both the cases at various inlet HTF velocities. Considering the quantity of PCM encapsulated in 49 spherical balls packed in the storage tank, the maximum heat energy that can be accounted in the TES tank is ~ 1700 kJ. It is seen from the figure that for the case I experiment conducted at the inlet HTF velocity of 1 m/s, the cumulative energy stored at the end of 610 minutes was only 1200 kJ. This shows that the tank is not completely charged which is also ensured from Fig. 5 (c), where the PCM placed at the last row of the TES tank does not reach the end solidification temperature. The cumulative energy stored in the case I experiment conducted at the HTF velocities of 2 m/s and 1.5 m/s was found to be 1820 kJ and 1900 kJ respectively. During the case I experimentations, the HTF temperature inside the TES tank is slightly higher than the ambient temperature because of the heat generated by the continuous operation of the fan. Hence, some heat energy from the TES tank was lost to the ambient. However, in case II experiments the figure indicates that cumulative energy stored is much greater than the storage capacity of the TES tank, particularly with the higher inlet velocities. This could be due to the fraction of cool energy carried away by the sprayed water particles, which is accounted as energy transferred to the PCM during the evaluation of instantaneous heat transfer.

"Fig. 10. Cumulative energy stored"

4.6. Fraction of total heat transfer

During the experimentation, only the inlet and outlet temperature of HTF at every 'i^{th}' time step was measured. In the present work, equation 6 was developed to find the HTF temperature

after each row of the TES tank. The developed equation was used to analyze the temperature distribution of the HTF across the TES tank and the heat transferred by the HTF to the PCM at each row of the TES tank. The temperature of the HTF evaluated after the 7th row was compared with the outlet temperature of the HTF measured during the experiments. The derived and measured HTF temperature at 2 m/s HTF velocity for both the cases are plotted in Fig. 11 and they are in good agreement.

"Fig. 11. Validation of derived HTF outlet temperature"

Fig. 12 (a) and (b) shows the fraction of heat energy transferred to the PCM at various rows of the TES tank for the case I and case II experiments respectively at the inlet HTF velocity of 2m/s. It is seen from Fig. 12 (a) that the heat transferred to all the rows of TES tank is nearly equal until the PCM in the 1st row is completely charged. Once the PCM in the 1st row got completely charged, it was not able to absorb further energy from the HTF and hence the fraction of heat transferred to the 1st row started to decline at a faster rate and this fraction of energy was transferred to the successive rows of the TES tank. Hence, a higher fraction of heat energy transferred was observed in the subsequent rows. However, in case II experiments there is an observable difference from the beginning of the experimentation until the PCM placed in the initial rows of the TES tank gets completely charged. This difference is due to the appreciable drop in the HTF temperature along the height of the storage tank. After the solidification of PCM placed in the initial rows, the fraction of heat transfer showed a similar trend as of the case I experiments.

"Fig. 12. Fraction of total heat energy transferred to the PCM placed at various location of TES tank at 2 m/s HTF velocity for (a) case 1 experiment (b) case II experiment"

5. Conclusion

In the present work, solidification behavior of PCM-based free cooling system integrated with and without direct evaporative cooling (DEC) unit was studied experimentally under real time moderate climatic conditions. The results obtained for the two cases are compared and the enhancement achieved in thermal performance of the storage tank through the hybrid concept is presented. One main advantage observed in the modified system is the increase in the potential of PCM-based free cooling system through the integration of evaporative cooling unit. An appreciable reduction in the charging duration was observed at all HTF velocities for the experiments conducted with modified free cooling system due to the reduction in inlet HTF temperature depending on the local relative humidity. It is construed from the results that the increase in HTF velocity has considerable effect in the conventional free cooling, whereas it has only a marginal effect in the integrated system. The instantaneous heat transfer during the sensible

cooling process is high for both the cases and it dropped at a faster rate within a shorter duration. Once the phase change of the PCM is initiated, a near uniform heat transfer rate is observed. However, the instantaneous heat transfer is uniformly higher for the experiments conducted with the integrated system. The experimental results obtained for the integrated system over predicts the cumulative energy stored particularly at the experiments conducted at the inlet HTF velocities of 2 and 1.5 m/s. This could be due to fraction of the cool energy carried away by the sprayed water particles, which is accounted as energy transferred to the PCM during the evaluation of instantaneous heat transfer. The fraction of total heat transferred to the various rows of PCM placed in the TES tank is used to illustrate the shift in the magnitude of heat transfer along the height of the storage tank with respect to time.

In continuation to the present work, there are further scope for the research to conduct various parametric analysis such as analyzing the effect of nozzle diameter, water droplets size, effect of geometry and material of the PCM encapsulations. This will give further insights to the research work and will optimize the thermal performance of the proposed modified cooling system. The results reported in the present work will be very useful for the building design engineers, architects towards adopting free cooling concept in buildings and designing energy efficient buildings. The modified free cooling system can be operated as a single stand-alone cooling system to meet the cooling demand of the buildings or it can be integrated with the mechanically operated HVAC systems to achieve energy efficiency in the overall cooling system.

Acknowledgement

The authors sincerely thank Inspire Fellowship program division (Fellowship no. DST/INSPIRE Fellowship/2013/568), Department of Science and Technology (DST), Government of India, for providing the necessary financial support through "Innovation in Science Pursuit for Inspired Research (INSPIRE) fellowship" for the Ph.D. program. The authors also express their heartful thanks to Indo-US Science and Technology Forum (IUSSTF) towards the funding rendered through Building Energy Efficiency in Higher & Advanced Network (BHAVAN) Internship (Internship no: IUSSTF BHAVAN Internships 2016/2/Karthik Panchabikesan). The first author sincerely thank Dr. Muthusamy V. Swami, Program Director, Buildings Division, Florida Solar Energy Centre, U.S.A. for his valuable comments towards this manuscript.

Nomenclature

$\dot{m}_f$	Mass flow rate of the air (kg. s^{-1})
A_{pcm}	Area of spherical ball (m^2)
$A_{TES\ section}$	Lateral surface area of the TES section (m^2)
$c_{p,\ HTF}$	Specific heat capacity of HTF (kJ. kg^{-1}. $°C^{-1}$)
D_p	Diameter of the PCM spherical encapsulation (m)
dt	Time duration (seconds)
h	Convective heat transfer coefficient ($W.m^{-2}$. $°C^{-1}$)
H_1 and H_2	Enthalpy of inlet and outlet HTF ((kJ. kg^{-1})
k_{HTF}	Thermal conductivity of HTF ($W.m^{-1}$. K^{-1})

$k_{insulation}$	Thermal conductivity of insulation ($W.m^{-1}.K^{-1}$)
n	number of spherical capsules in each row of TES tank
Nu	Nusselt number
Pr	Prandtl number
Q_c^i	Instantaneous cumulative energy stored (Kj)
$\dot{Q}_{ins}$	Instantaneous heat transfer (kW)
Q^i_{loss}	Instantaneous heat loss (Kw)
Re	Reynolds number
S_v	ratio between area and volume of the spherical capsule (m^{-1})
T	Temperature (°C)
T_l	onset solidification temperature of PCM (°C)
T_s	end freezing temperature of PCM (°C)
v_s	superficial velocity ($m.s^{-1}$)
x	thickness of insulation (m)

Subscripts

HTF	heat transfer fluid
HTF,in	HTF at the entry of TES tank
HTF,out	HTF at the exit of TES tank
j, HTF	HTF at the j^{th} location of the TES tank

Superscripts

i	time step

Greek symbols

ε	porosity of TES tank
μ	dynamic viscosity of the HTF ($kg.m^{-1}.s^{-1}$)
ρ	density of HTF ($kg.m^{-3}$)

Abbreviations

CFM	Cubic feet per minute
DEC	Direct evaporative cooling
DSC	Differential scanning calorimetry
GPH	Gallon per hour (U.S. equivalent)
HDPE	High-density polyethylene
HP	Horse power
HTF	Heat transfer fluid
HVAC	Heating ventilation and air conditioning
MT DSC	Mettler Toledo differential scanning calorimetry
OD	Outer diameter

PCM	Phase change material
RH	Relative humidity
RT	Rubitherm
RTD	Resistance temperature detector
TES	Thermal energy storage

References

1. Smita C, Rajan R. Building Policies for a Better World. . Building Policies for a Better World: Global Buildings Performance Network (GBPN); 2013. http://www.gbpn.org/activities/india, Accessed on June 10, 2017
2. Souayfane F, Fardoun F, Biwole P-H. Phase change materials (PCM) for cooling applications in buildings: A review. Energy and Buildings. 2016;129:396-431.
3. Raj VAA, Velraj R. Review on free cooling of buildings using phase change materials. Renewable and Sustainable Energy Reviews. 2010;14(9):2819-29.
4. Waqas A, Ud Din Z. Phase change material (PCM) storage for free cooling of buildings—A review. Renewable and Sustainable Energy Reviews. 2013;18:607-25.
5. Osterman E, Tyagi VV, Butala V, Rahim NA, Stritih U. Review of PCM based cooling technologies for buildings. Energy and Buildings. 2012;49:37-49.
6. Kamali S. Review of free cooling system using phase change material for building. Energy and Buildings. 2014;80:131-6.
7. Thambidurai M, Panchabikesan K, N KM, Ramalingam V. Review on phase change material based free cooling of buildings—The way toward sustainability. Journal of Energy Storage. 2015;4:74-88.
8. Panchabikesan K, Vellaisamy K, Ramalingam V. Passive cooling potential in buildings under various climatic conditions in India. Renewable and Sustainable Energy Reviews. 2017;78:1236-52.
9. Alizadeh M, Sadrameli SM. Development of free cooling based ventilation technology for buildings: Thermal energy storage (TES) unit, performance enhancement techniques and design considerations – A review. Renewable and Sustainable Energy Reviews. 2016;58(Supplement C):619-45.
10. Zalba B, Marín JM, Cabeza LF, Mehling H. Free-cooling of buildings with phase change materials. International Journal of Refrigeration. 2004;27(8):839-49.
11. Stritih U, Butala V. Experimental investigation of energy saving in buildings with PCM cold storage. International Journal of Refrigeration. 2010;33(8):1676-83.
12. Antony Aroul Raj V, Velraj R. Heat transfer and pressure drop studies on a PCM-heat exchanger module for free cooling applications. International Journal of Thermal Sciences. 2011;50(8):1573-82.
13. Arkar C, Medved S. Free cooling of a building using PCM heat storage integrated into the ventilation system. Solar Energy. 2007;81(9):1078-87.
14. Arkar C, Vidrih B, Medved S. Efficiency of free cooling using latent heat storage integrated into the ventilation system of a low energy building. International Journal of Refrigeration. 2007;30(1):134-43.
15. Liu S, Iten M, Shukla A. Numerical study on the performance of an air—Multiple PCMs unit for free cooling and ventilation. Energy and Buildings. 2017;151(Supplement C):520-33.

16. Medved S, Arkar C. Correlation between the local climate and the free-cooling potential of latent heat storage. Energy and Buildings. 2008;40(4):429-37.
17. Vidrih B, Arkar C, Medved S. Generalized model-based predictive weather control for the control of free cooling by enhanced night-time ventilation. Applied Energy. 2016;168(Supplement C):482-92.
18. Mosaffa AH, Garousi Farshi L, Infante Ferreira CA, Rosen MA. Energy and exergy evaluation of a multiple-PCM thermal storage unit for free cooling applications. Renewable Energy. 2014;68:452-8.
19. Solomon GR, Karthikeyan S, Velraj R. Sub cooling of PCM due to various effects during solidification in a vertical concentric tube thermal storage unit. Applied Thermal Engineering. 2013;52(2):505-11.
20. Muthuvelan T, Panchabikesan K, Munisamy R, Nibhanupudi KM, Ramalingam V. Experimental investigation of free cooling using phase change material-filled air heat exchanger for energy efficiency in buildings. Advances in Building Energy Research. 2016:1-11.
21. Sparrow EM, Schmidt RR, Ramsey JW. Experiments on the Role of Natural Convection in the Melting of Solids. Journal of Heat Transfer. 1978;100(1):11-6.
22. Velraj R, Seeniraj RV, Hafner B, Faber C, Schwarzer K. Heat transfer enhancement in a latent heat storage system. Solar Energy. 1999;65(3):171-80.
23. Ismail KAR, Alves CLF, Modesto MS. Numerical and experimental study on the solidification of PCM around a vertical axially finned isothermal cylinder. Applied Thermal Engineering. 2001;21(1):53-77.
24. Solomon GR, Velraj R. Analysis of the heat transfer mechanisms during energy storage in a Phase Change Material filled vertical finned cylindrical unit for free cooling application. Energy Conversion and Management. 2013;75:466-73.
25. Stritih U. An experimental study of enhanced heat transfer in rectangular PCM thermal storage. International Journal of Heat and Mass Transfer. 2004;47(12–13):2841-7.
26. Castell A, Solé C, Medrano M, Roca J, Cabeza LF, García D. Natural convection heat transfer coefficients in phase change material (PCM) modules with external vertical fins. Applied Thermal Engineering. 2008;28(13):1676-86.
27. Agyenim F, Eames P, Smyth M. A comparison of heat transfer enhancement in a medium temperature thermal energy storage heat exchanger using fins. Solar Energy. 2009;83(9):1509-20.
28. Kumaresan V, Velraj R, Das SK. The effect of carbon nanotubes in enhancing the thermal transport properties of PCM during solidification. Heat and Mass Transfer. 2012;48(8):1345-55.
29. Zeng JL, Cao Z, Yang DW, Sun LX, Zhang L. Thermal conductivity enhancement of Ag nanowires on an organic phase change material. Journal of Thermal Analysis and Calorimetry. 2010;101(1):385-9.
30. Liu Y-D, Zhou Y-G, Tong M-W, Zhou X-S. Experimental study of thermal conductivity and phase change performance of nanofluids PCMs. Microfluidics and Nanofluidics. 2009;7(4):579.
31. Chandrasekaran P, Cheralathan M, Velraj R. Effect of fill volume on solidification characteristics of DI (deionized) water in a spherical capsule – An experimental study. Energy. 2015;90, Part 1:508-15.
32. Walsh BP, Murray SN, O'Sullivan DTJ. Free-cooling thermal energy storage using phase change materials in an evaporative cooling system. Applied Thermal Engineering. 2013;59(1–2):618-26.

33. Jaber S, Ajib S. Novel cooling unit using PCM for residential application. International Journal of Refrigeration. 2012;35(5):1292-303.
34. RT 28 HC data sheet. 2016. https://www.rubitherm.eu/media/products/datasheets/Techdata_-RT28HC_EN_31052016.PDF, Accessed on June 10, 2017.
35. Felix Regin A, Solanki SC, Saini JS. An analysis of a packed bed latent heat thermal energy storage system using PCM capsules: Numerical investigation. Renewable Energy. 2009;34(7):1765-73.
36. Strupstad A. Error Analysis of Flow Experiments. 2009.

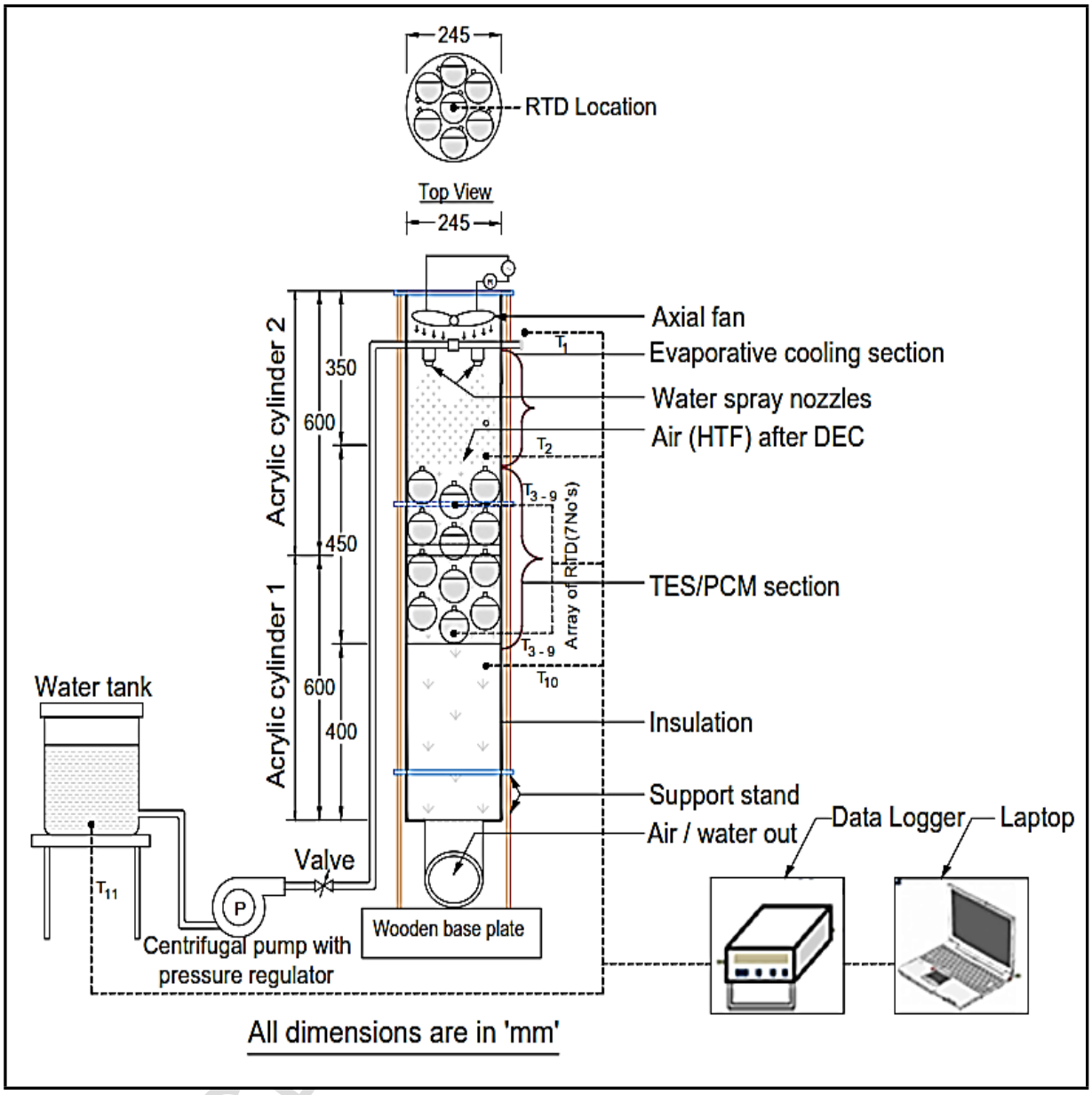

Fig. 1. Schematic diagram of modified free cooling system integrated with DEC unit

Fig. 2. Photographic views of **(a)** modified free cooling system without insulation, **(b)** water spray nozzle, **(c)** axial fan placed at the top of the TES tank, **(d)** Data acquisition system

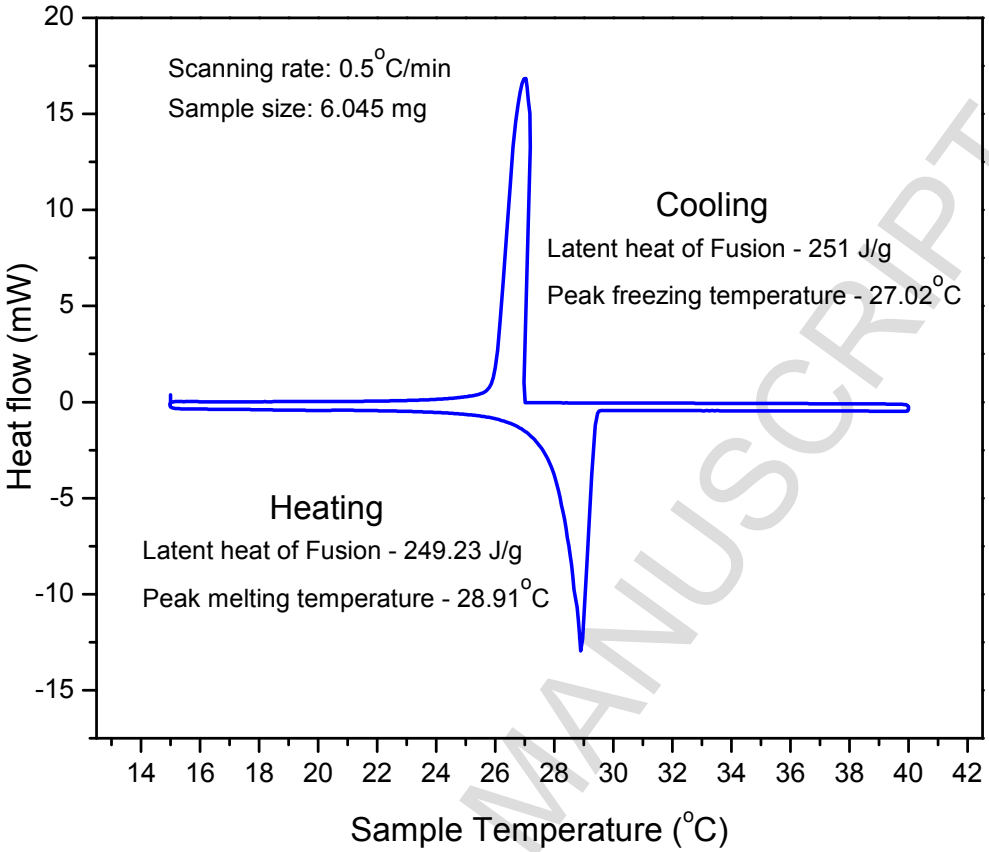

Fig. 3. DSC Analysis of paraffin (RT 28 HC)

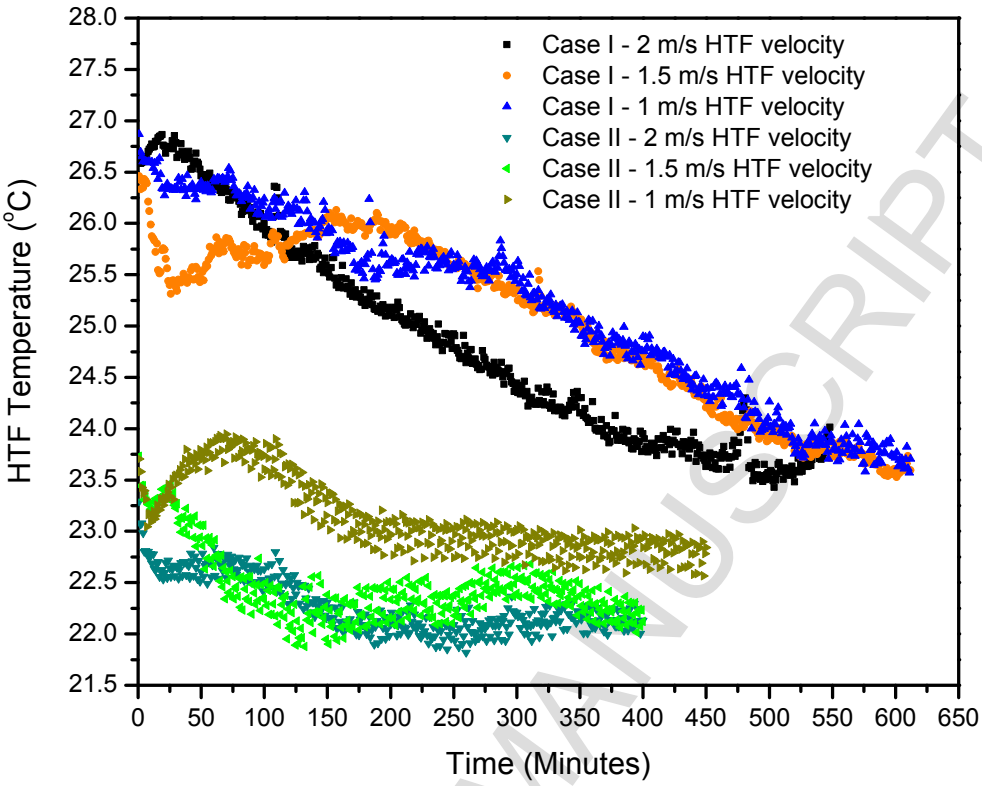

Fig. 4. Variation in HTF inlet temperature at various HTF velocities

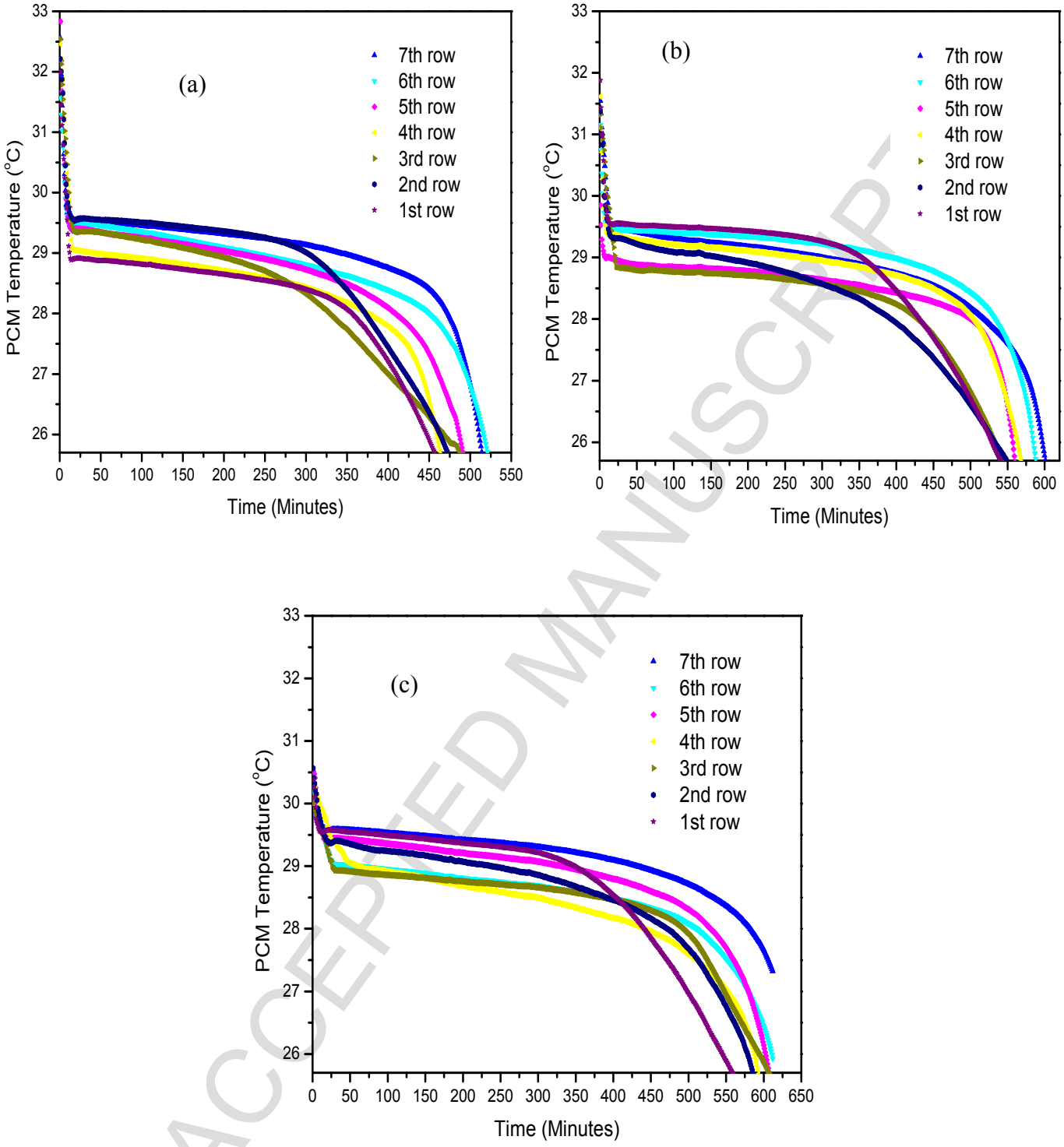

Fig. 5. Temperature-time history of PCM for the free cooling experiments conducted without the operation of DEC unit (a) 2 m/s velocity, (b) 1.5 m/s velocity, (c) 1 m/s velocity

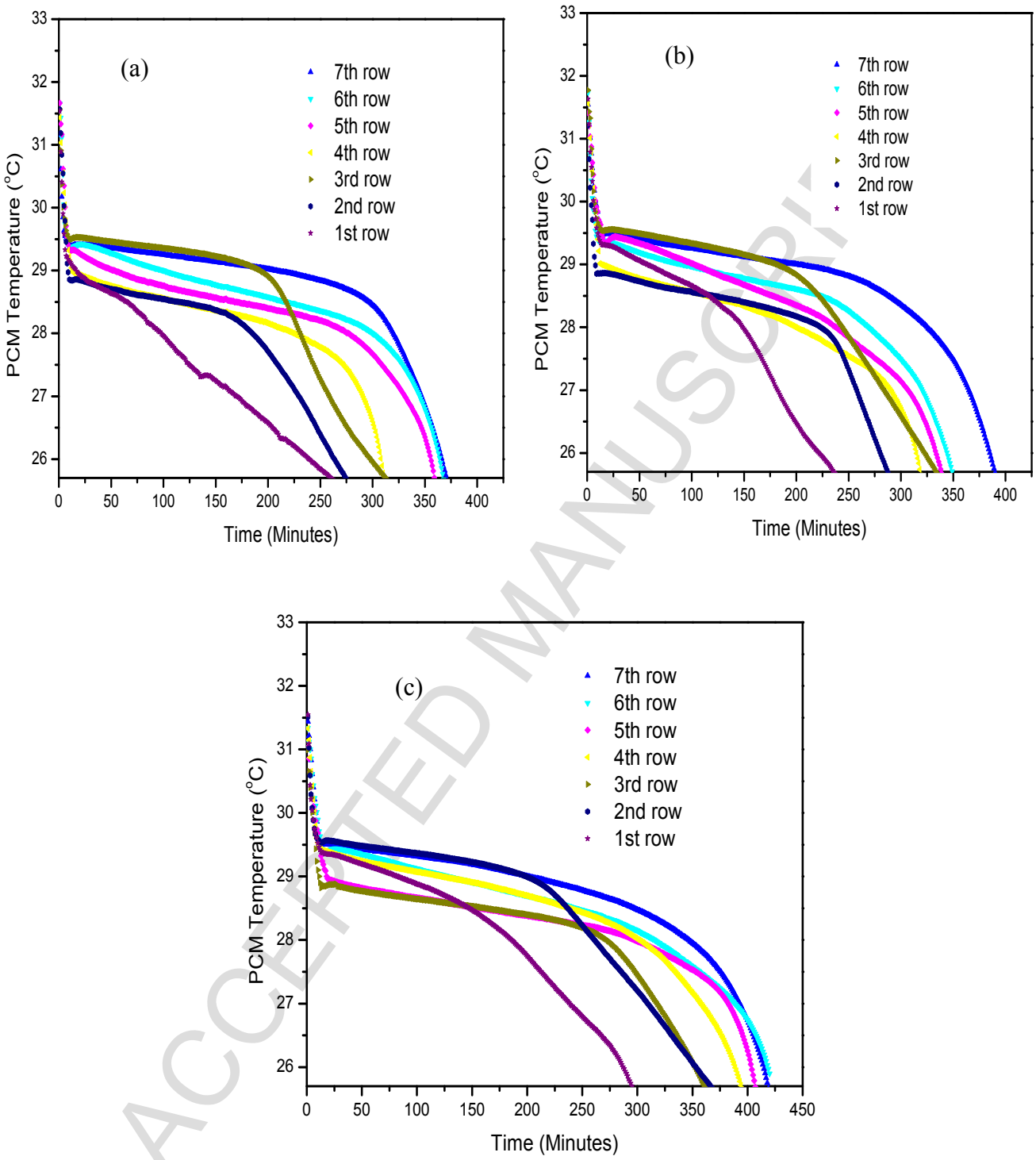

Fig. 6. Temperature-time history of PCM for the free cooling experiments conducted with the operation of DEC unit (a) 2 m/s velocity, (b) 1.5 m/s velocity, (c) 1 m/s velocity

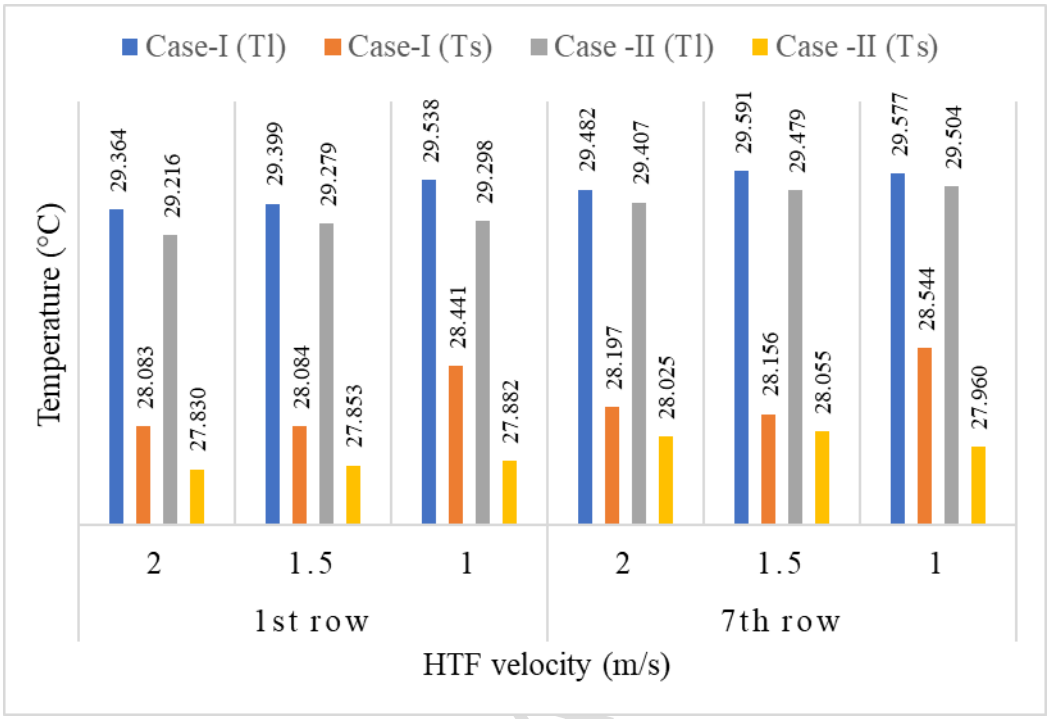

Fig. 7. Onset (T_l) and solidification (T_s) temperature of the chosen PCM obtained during the case I and II experimentations at 2, 1.5 and 1 m/s inlet HTF velocities.

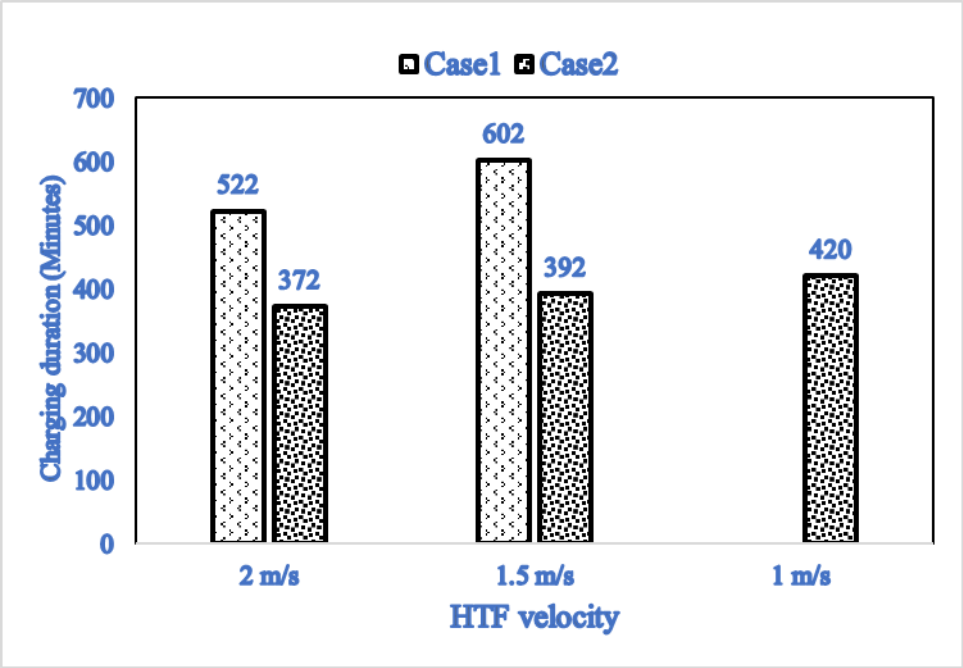

Fig. 8. Charging duration of the PCM placed at the last row of TES tank

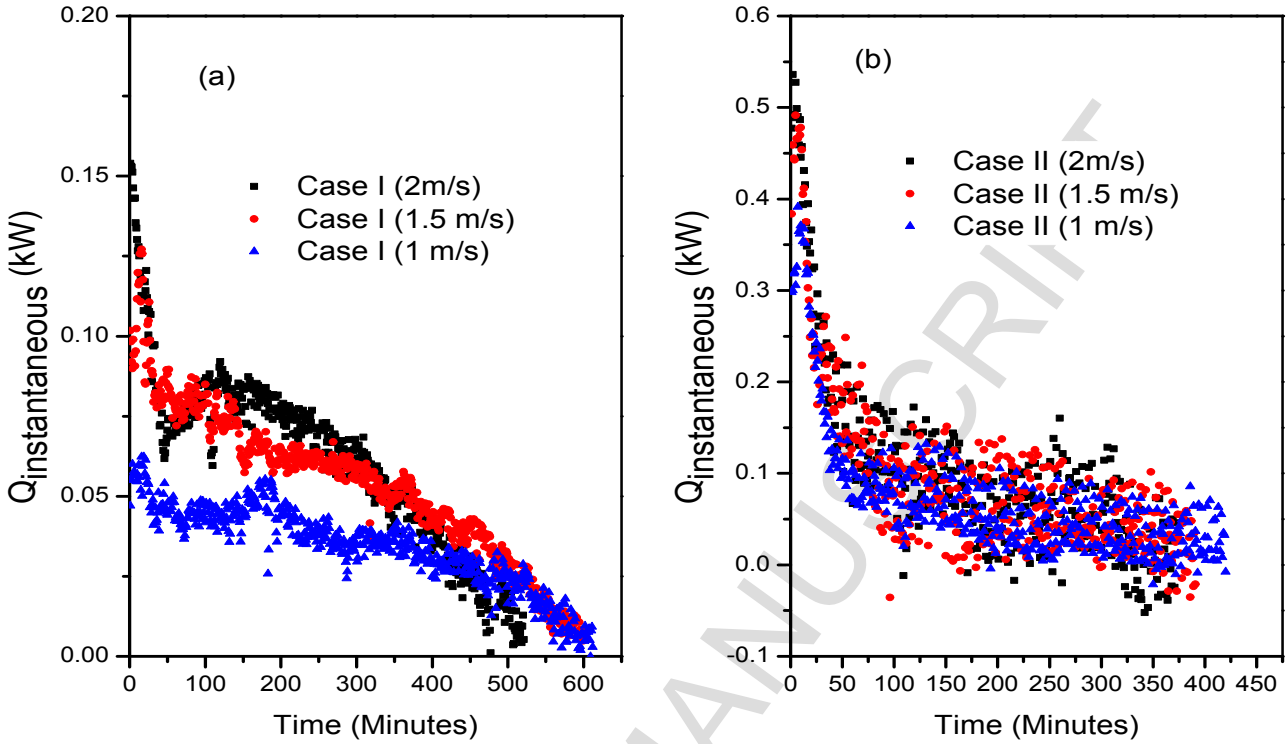

Fig. 9. Instantaneous heat transfer at various HTF velocities for (a) case I experiments (b) case II experiments

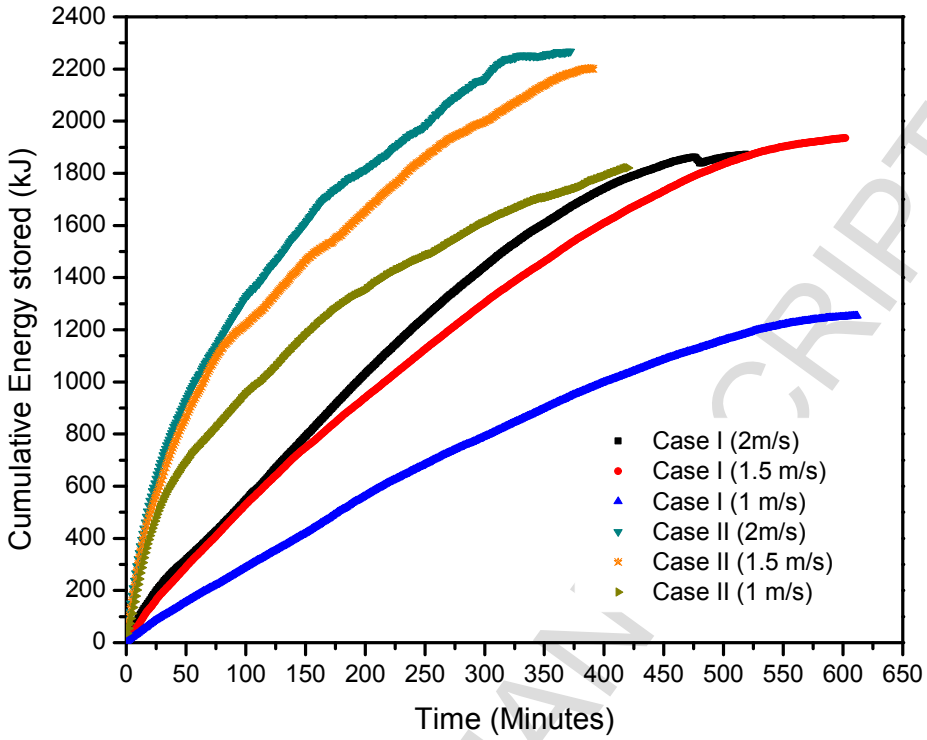

Fig. 10. Cumulative energy stored

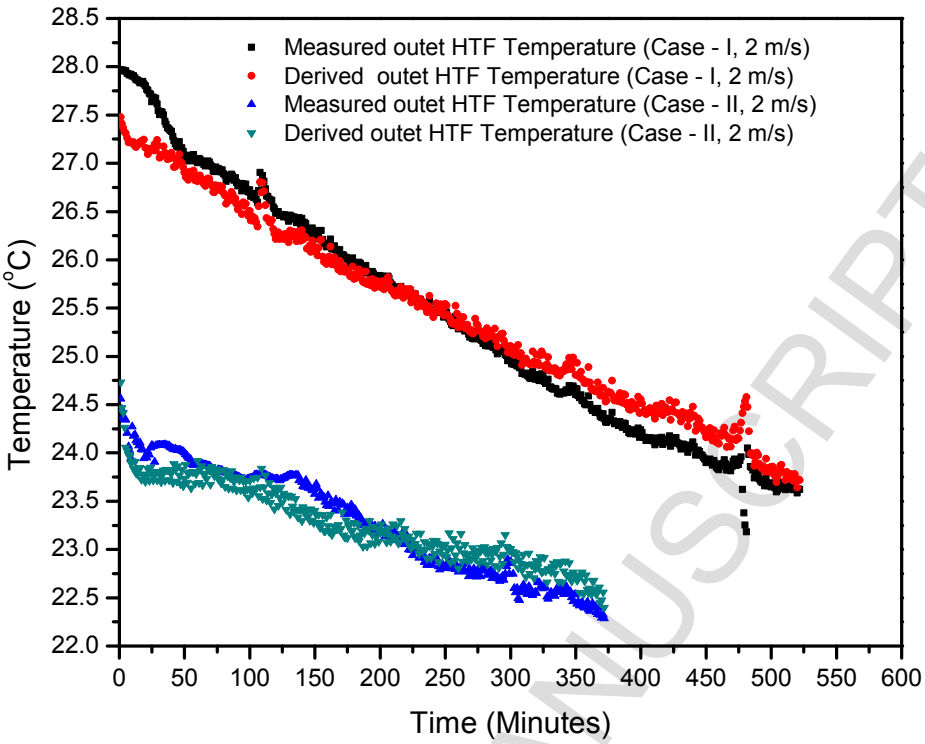

Fig. 11. Validation of derived HTF outlet temperature

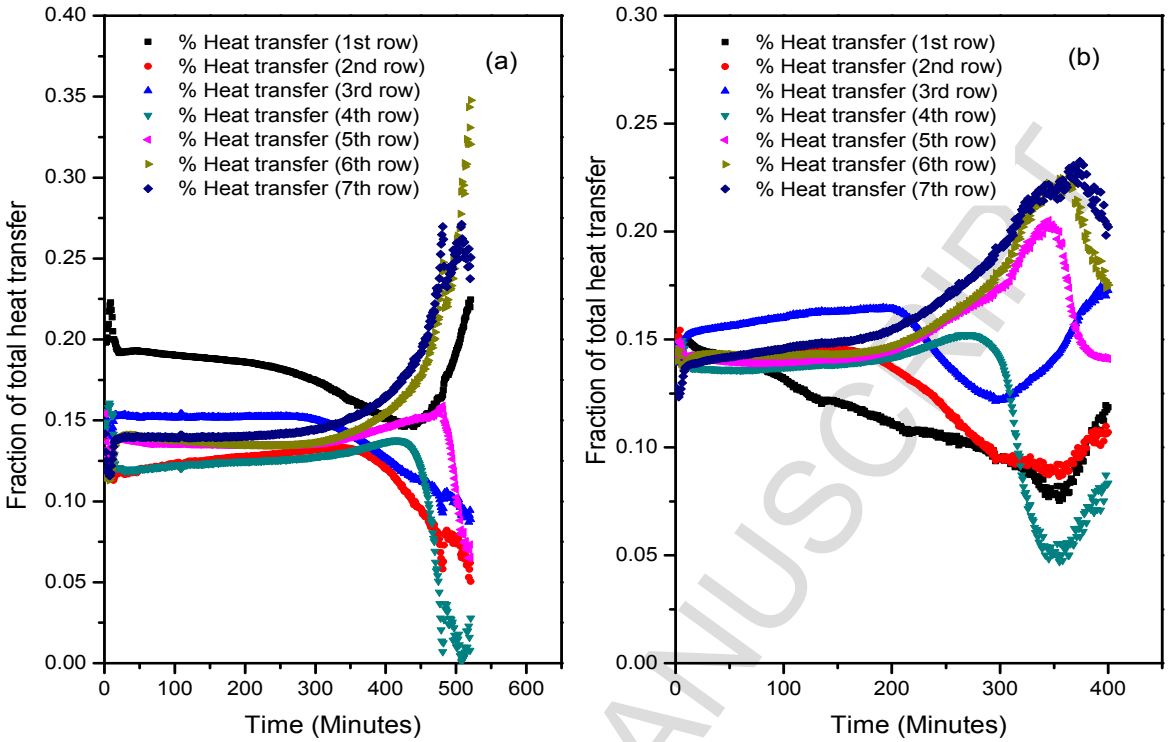

Fig. 12. Fraction of total heat energy transferred to the PCM placed at various location of TES tank at 2 m/s HTF velocity for (a) case 1 experiment (b) case II experiment

Table 1

Thermophysical properties of RT 28HC PCM [34]

Property	**Value**	**Unit**
Solidification Onset temperature*	27.07	°C
Peak temperature*	27.03	°C
End temperature	25.61	°C
Latent heat of fusion*	251	J/g
Specific heat	2000	J/g. K
Thermal Conductivity (Solid)	0.2	W/m.K
Thermal Conductivity (Liquid)	0.2	W/m.K
Density @ 15°C (solid)	880	kg/m^3
Density @ 40°C (liquid)	770	kg/m^3
Maximum operating temperature	50	°C
Volume expansion	12.5	%

* Data obtained from DSC results

Table 2
Uncertainty in measured and derived parameters

Measured Parameters	
Temperature	±0.46%
Mass flow rate	±3.72%
Time measurement	±0.27%
Derived parameters	
Convective heat transfer coefficient	±4.34%
Instantaneous heat transfer (case I)	±3.76%
Instantaneous heat transfer (case II)	±4.61%
Cumulative energy stored (case I)	± 3.77%
Cumulative energy stored (case II)	±4.68%
Heat loss	± 0.87%
HTF temperature at respective row	±4.93 %

Table 3
Comparison of inlet HTF conditions for different experimental trials

Experimental configuration	HTF velocity (m/s)	Relative Humidity (average) (%)	Ambient temperature (average) (°C)	Inlet air temperature (average) (°C)	Outlet air temperature (average) (°C)	Temperature driving potential (°C)	Convective heat transfer coefficient ($W.m^{-2}.°C^{-1}$)
Case I	2	85.6	23.82	24.88	25.40	2.12	16.34
	1.5	83.72	23.75	25.04	25.64	1.96	13.83
	1	85.54	23.86	25.26	25.71	1.74	10.96
Case II	2	81.3	24.54	22.29	23.28	4.71	18.89
	1.5	80.8	24.81	22.46	23.58	4.54	16.00
	1	81.3	24.51	23.15	23.88	3.85	12.69